Development of the Dynamic Simulation Program of a Multi-Inverter Heat Pump under Frosting Conditions

Byung-Duck Park†, Joo-Dong Lee*, Baik-Young Chung**

School of Mechanical Engineering, Sangju National University, Sangju 742-178, Korea

**Samsung Electronics Co. Ltd., Air Conditioning R&D Team, Suwon 443-742, Korea*

***LG Electronics Inc., Digital Appliance Research Laboratory, Seoul 153-023, Korea*

Key words: Frosting, Multi-inverter heat pump, Transient, Dynamic simulation

ABSTRACT: In case of heat exchangers operating under frosting condition, the thermal resistance and the air-side pressure loss increase with a growth of frost layer. In this paper, a transient characteristic prediction model of the heat transfer for a multi-inverter heat pump with frosting on its surface was presented by taking into account the change of the fin efficiency due to the growth of the frost layer. This dynamic simulation program was developed for a basic air conditioning system composed of an evaporator, a condenser, a compressor, a linear electronic expansion valve, and a bypass circuit. The theoretical model was derived from measured heat transfer and mass transfer coefficients. We also considered that the heat transfer performance was only affected by the decrease of wind flow area. The calculated results were compared with the experimental results for frosting conditions.

Nomenclature

a_F : surface area of fin [m^2]
a_p : surface area of tube [m^2]
C_p : air specific heat at constant pressure [kJ/kgK]
d_i : diameter [m]
f : friction coefficient [-]
Fr : Froude number [-]
G_a : air mass flow [kg/min]
G_r : refrigerant mass flow rate [kg/m^2s]
h : air side heat transfer rate [W/m^2K]
h_D : air side mass transfer rate [kg/m^2s]
h_w : heat transfer rate in tube [W/m^2K]
L : length [m]
m : mass [kg]
n : number of band returned
Nu : Nusselt number [-]
P : pressure [MPa]
Pr : Prandtl number [-]
ΔP : windage loss [Pa]
Q : heating capacity [kW]
q : heat flow rate in air side [kW/m^2]
q' : refrigerant side heat flow rate [kW/m^2]
Re : Reynolds number [-]
t : air temperature [K], time lapsed for frosting [sec]
t_f : surface temperature of frost layer in fin [K]
t_p : surface temperature of frost layer in tube [K]
t_s : surface temperature of fin [K]
Δt_w : temperature change of refrigerant [K]
U_f : wind speed per unit throughout area [m/s]

† Corresponding author
Tel.: +82-54-530-5335; fax: +82-54-530-5407
E-mail address: bdpark@sangju.ac.kr

x : absolute humidity in air [kg/kg'], degree of dryness [-]
x_f : absolute humidity of frost layer in fin [kg/kg']

Greek symbols

δ_f : growth of frost layer [m]
γ : latent heat [kJ/kg]
ρ : density [kg/m^3]
ρ_f : density of frost layer [kg/m^3]
λ_F : thermal conductivity of fin [W/mK]
λ_f : thermal conductivity of frost layer [W/mK]
ϕ : fin efficiency [-]
Φ : Lockhard-Martinelli parameter [-]
ζ : non-directional resistance coefficient [-]

Subscripts

1 : air in
2 : air out
$c1$: surface inside tube
$c2$: surface outside tube
l : liquid phase
m : average mix
sh : degree of superheat [K]
$w1$: refrigerant in
$w2$: refrigerant out

1. Introduction

Air conditioning has been widely used with the increase of per capita income. When an air conditioner of older design is used in a room, the temperature of the room is maintained by compressor on-and-off. Because great torque is required for the compressor on-and-off, this control scheme is not desirable in the aspect of energy efficiency. The air conditioner with an inverter compressor, could improve energy efficiency, in a lot easier way than that of the conventional air conditioning unit in which the compressor runs at a fixed speed. The swing of room temperature could be minimized with the inverter compressor air-conditioner, and, it improves the quality of thermal comfort, so that the air-conditioner with inverter compressor is widely used.

Recently, people tend to have air-conditioners in each room, instead of having only one air-conditioner in a house. For commercial use, multi-evaporator type air-conditioners are preferred for the higher energy efficiency. Multi-type air conditioners are usually for both heating and cooling and it could replace boiler for heating and save installation space. For the multi-type air-conditioner, there could be various configurations of connecting indoors units of different capacity to an outdoor unit, so that lots of experimental data are required to cope with the various configurations and operating conditions. Refrigerant flow rate, heat transfer rate, and other system parameters are to be measured to stabilize the operation of the multi-type air-conditioner. Thus it requires enormous amounts of tests for designing the air-conditioner. The performance analysis of the air-conditioner is required in designing components of the system and optimizing the system parameters. Park et al.[1-2] carried out a study on the performance analysis of the multi-type air-conditioner for heat pumping operation. They determined the control mode for defrosting, based only on experimental data, without analyzing system behavior in detail, when frosting and defrosting occurred.

Many researches and studies[3-7] have been performed to analyze the progress of frosting and the heat transfer characteristics for heat exchangers, but there are only a few research works regarding interpretation of the operating characteristics of the air-conditioner heat pump accompanying frosting, which had been done by Aoki.[8]

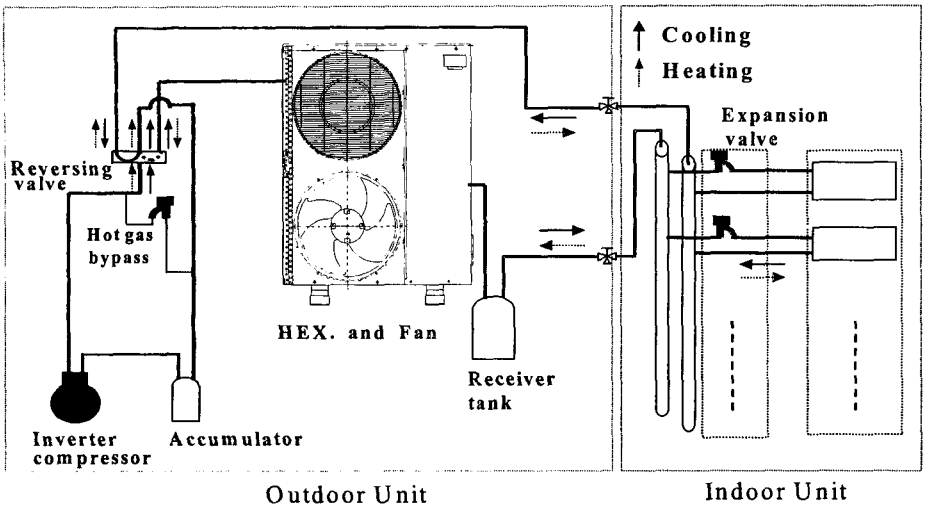

Fig. 1 Schematic diagram of a multi-heat pump system.

In this research, we developed a model for predicting the performance of air-conditioner in heat pumping mode. We considered the effects of frost accumulation on the heat transfer performance of heat exchangers and subsequently on the system performance. Also, we developed a program based on this result, for designing multi-type air-conditioners to determine control factors.

We developed the program using Visual Basic 6.0, and this program offers graphic user interface for easy access, and R22 refrigerant is considered.

2. Frosting modeling

Figure 1 shows the schematic diagram of a multi heat pump system that used for performance analysis. The system is composed of an outdoor unit and several indoor units. The outdoor unit consists of a compressor, a heat exchanger (condenser or evaporator), a fan, a receiver, an oil separators, a 4-way valve, and each of the indoor units consists of a heat exchanger (condenser or evaporator), a fan, an expansion valve. As for the compressor, we used inverter type scroll compressor, and as for the heat exchanger, we used fin-tube heat exchanger. Particularly we adopted linear electronic expansion valve (EEV), which makes the opening of the expansion valve change according to the number of electrical pulse. In this study, we examined the transient situations of the analysis model using Okawa's[9] model having considered only for the basic components

Table 1 Specifications of the multi inverter heat pump unit

Component		Specification
Outdoor unit	Compressor	Scroll type Frequency : 30~110 Hz
	Heat exchanger	Plate fin and tube type
Indoor unit	A Type	Capacity : 2.3 kW
	B Type	Capacity : 3.3 kW
	C Type	Capacity : 4.1 kW

Table 2 A specification of outdoor unit

Type	2 lines, 44 rows
Tube arrangement	In line
Tube outer diameter	9.50 mm
Tube row pitch	19.05 mm
Tube line pitch	25.4 mm
Fin thickness	0.105 mm
Fin pitch	1.59 mm

that have great impacts on the performance of the system. The system components are described in Table 1, and Table 2 shows the specification of outdoor unit that used in the simulation.

With frost accumulation, the thermal resistance of the heat exchanger increases, and heat transfer and mass transfer characteristics change with time along with blocking the air-passage of the heat exchanger. In this research, we examined the performance of heat transfer when frosting with calculation of the heat transfer coefficient and the mass transfer coefficient independently. As to the impact of the frosting on the performance of heat transfer, we only considered the fact that the flow path in air-side was reduced.

In this frosting model, the fin-tube heat exchanger has been simplified, the airflow and the flow of coolant in tube are crossing perpendicularly, and the temperature of the air at the inlet including humidity, and the temperature of the air at the outlet including humidity are different in isolated spots.

In the model as shown in Fig. 2, this has been treated as a heat transfer tube, and each interval between fins has been considered as a factor, and the state of air is changing from t_1, x_1 to t_2, x_2 and the temperature of refrigerant is changing as much as Δt_w. For model development, we made following assumptions:

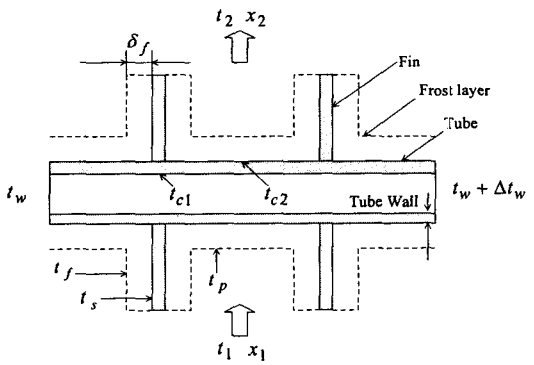

Fig. 2 Schematic of simulation model for the fin and tube type HEX.

(1) Thickness of frosting is uniform on both tubes and fins.

(2) Surface temperature inside tube, t_{c1}, surface temperature of tube, t_{c2}, surface temperature of fin, t_s, are uniform for each surface.

(3) Refrigerant-side heat transfer coefficient, h_w, mass transfer coefficient, h_D, Air-side heat transfer coefficient, h, are uniform respectively.

(4) Thermal conductivity of frost layer, λ_f is considered to be determined only by density of frost layer, ρ_f.

(5) Velocity of frosting is considered slow and phenomena of frosting are considered as quasi-transient state.

(6) Air on the surface of frost layer is in a saturated state.

With the above assumptions, we derived a correlating equation for each part of the fin. Also the refrigerant in the heat exchanger exists in either single-phase of gas/liquid or mixture of liquid and gas, according to cooling or heating operation and its operation cycle. For each and every phase, we applied different heat transfer coefficients and pressure drop correlations. Hereby, the heat transfer coefficient correlation and pressure drop correlation were developed within the error bounds of max ±21% and ±35%, respectively from the experimental data.

Correlation in fin

Eq. (1) below shows the heat and mass transfer correlations of frost layer in fins.

$$h(t-t_f)+h_D\gamma(x-x_f)=\lambda_f\frac{t_f-t_s}{\delta_f} \qquad (1)$$

At fin, the correlation between t_f and t_s, are shown in Eq. (1). Relation between t_{c2} and t_f are expressed as Eq. (2) below.

$$\phi=\frac{\int h(t-t_f)\,da_F+\int h_D\gamma(x-x_f)\,da_F}{\int h(t-t_{c2})\,da_F+\int h_D\gamma(x-x_{c2})\,da_F} \qquad (2)$$

In Eq. (2), the numerator represents actual amount of heat exchanges, and the denominator represents the amount of heat exchanges at the time when the surface temperature of fin is the same as the root temperature of fin, t_{c2}. And the fin efficiency will be determined if heat transfer coefficient, h, and mass transfer coefficient, h_D, are already known values. If the fin efficiency is determined, correlation between t_f and t_{c2} is to be obtained. By using the above correlations, the correlations between t_f, t_s and t_{c2} are to be determined.

Correlation in tube

Eq. (3) below shows the equation for the heat transfer of the frost layer in tubes.

$$h(t-t_p)+h_D\gamma(x-x_p)=\frac{\lambda_f}{\delta_f}(t_p-t_{c2}) \quad (3)$$

Using above Eq. (3), the equation for temperature and absolute humidity in saturation are to be approximated to linear expressions as Eqs. (4), (5) and (6) in order to induce the relationship between the surface temperature of tube, t_p and the root temperature of fin, t_{c2}, and also the relationship between the surface humidity of tube, x_p and the surface humidity of fin root, x_{c2}.

$$t=P_1x+P_2 \quad (P_1,\ P_2 : \text{Parameter}) \quad (4)$$

$$t_p=P_1x_p+P_2 \quad (5)$$

$$t_{c2}=P_1x_{c2}+P_2 \quad (6)$$

In Eq. (6), if the relationship between the root temperature of fin, t_{c2} and the root humidity of fin, x_{c2} can be expressed as a linear expression of P_1 and P_2, and then, in Eq. (4), the air temperature between fins, t and the air humidity, x can be approximated. And also in Eq. (5), the surface temperature, t_p and the surface humidity of tube, x_p can be calculated in the same way.

Equation for heat transfer in air side

Quantity of heat exchanged, q, in the air side is:

$$q=G_aC_p(t_1-t_2)+G_a\gamma(x_1-x_2) \quad (7)$$

Equation for heat transfer in refrigerant side

Heat quantity of refrigerant, q', which received from the wall of tube is:

$$q'=h_wa_p(t_{c1}-t_w) \quad (8)$$

Thermal conductivity of frost layer

The thermal conductivity of frost layer, λ_f, depends largely on the structure of frost. There was a difficulty that does not allow us to get the thermal conductivity according to the height of frosting by experiment. We used the empirical correlation of Ishihara,[10] which had been developed within error tolerance limits of $\pm 15 \sim \pm 20\%$ from the experimental results.

3. Calculation method

In the model applied to Fig. 2, the values not known yet are finally the growth of frost layer, δ_f and the temperatures, t_{c1}, t_{c2}, t_p, t_f. The saturated humidity, x_p and x_f can be calculated from the psychrometric chart after determining t_p, t_f. By using the equations described in the previous passages, the unknown quantities become three, those are, air heat transfer coefficient, h and mass transfer coefficient, h_D and δ_f.

In Fig. 3, we showed the flow chart of the present simulation. The followings show each step:

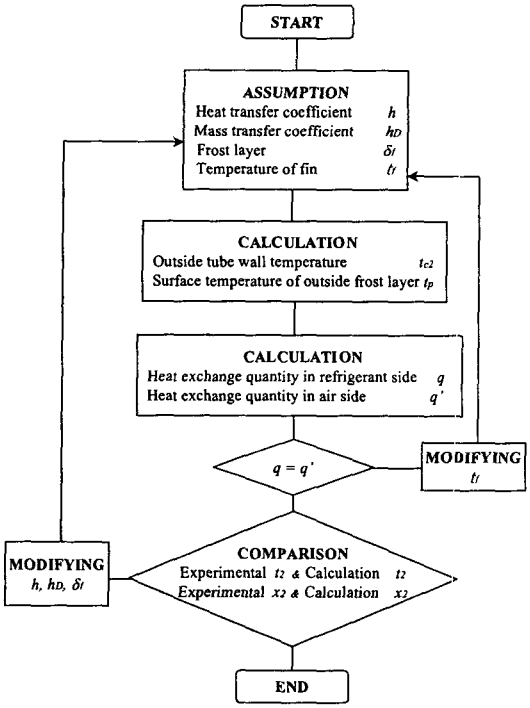

Fig. 3 Flow chart of a present simulation.

(1) Input the values that have been obtained from the experiments.

(2) Assume the growth of frost layer, δ_f.

(3) Assume the heat transfer coefficient, h, and the mass transfer coefficient, h_D.

(4) Assumed t_f, the surface temperature of frost layer in fin parts according to h, and the mass transfer coefficient, h_D, that assumed.

(5) Calculate the temperature of fin in frost layer t_{c2} and the temperature of fin t_p.

(6) Repeat the processes (2)~(5) according to each micro element.

(7) Repeat the above processes (2)~(5) until the time of accomplishing the balance between heat exchange quantity in air side according to heat transfer coefficient, mass transfer coefficient, temperature of fin, calculated temperature of fin, and temperature of fin parts that assumed, and heat exchange quantity in refrigerant side.

(8) If the balance of heat exchange quantity between air and refrigerant side has been achieved, verify the agreement between calculated and experimental values.

(9) Store the growth of frost layer, δ_f, and conclude the calculation.

(10) If the calculated values do not agree with the experimental ones, then return to the step (2) and assume the growth of frost layer, δ_f, newly and repeat entire procedures.

4. Results and discussions

Using the theoretical model as described in the previous chapter, we made a comparison between the experimental and calculated results with regard to frosting phenomena of multi inverter heat pump. These results had been obtained from the modification of the connecting method of indoor units and the conditions of air.

The system used in the experiments is the same as Fig. 1 that used in the model. The experiments were implemented having installed multi type psychrometric chamber, which had numbers of indoor units. We executed the experiments that concerned with the response characteristics of transient and steady state under 2.0/0.8℃ and 2.0/1.5℃ of dry-bulb and wet-bulb temperatures, respectively. These conditions of frosting and defrosting were based on the KS9306.[11] And the experimental data had been measured within the error tolerance limits of ±3.0%.

Figures 4, 5, 8, and 9 exhibit condensing and evaporating pressure (Fig. 4), heating capacity (Fig. 5), air mass flow rate (Fig. 8) and the growth of the frost layer (Fig. 9) each when operating 2 units of A type heat exchanger and 2 units of B type heat exchanger having connected together. We operated it with 70 pulses in case of a type, and 100 pulses in case of B type and 80 pulses in case of C type as the opening of electronic expansion valve. When we started the compressor, the

frequency of 30 Hz was used, and after about 2 minutes, we operated it with increase of frequency up to 105 Hz, which was the target frequency.

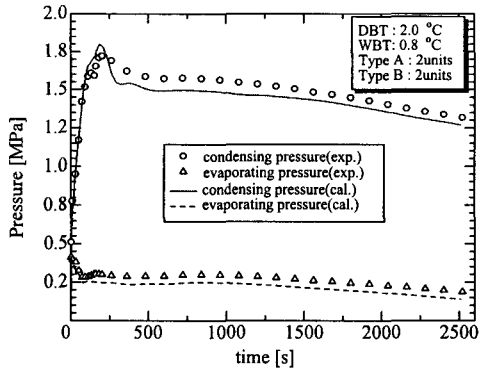

Fig. 4 The pressure characteristic at DB/WB =2.0/0.8℃.

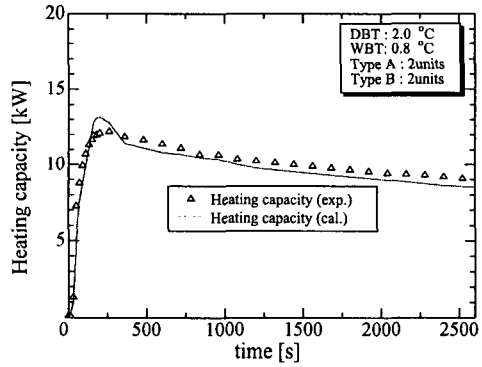

Fig. 5 The heating capacity at DB/WB=2.0/ 0.8℃.

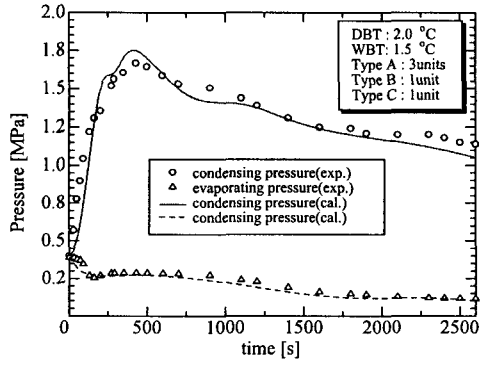

Fig. 6 The pressure characteristic at DB/WB =2.0/1.5℃.

4.1 Pressure characteristics and heating capacity

Figure 4 shows the comparison between the

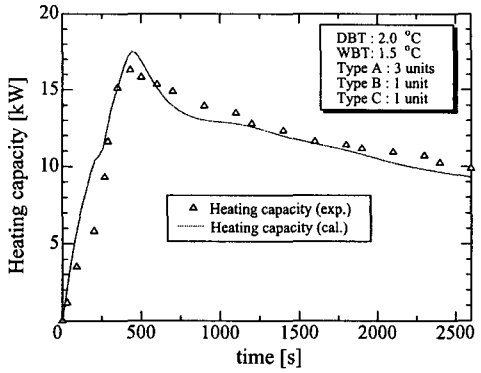

Fig. 7 The heating capacity at DB/WB=2.0/ 1.5℃.

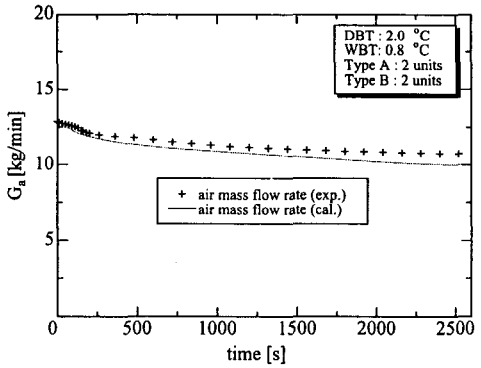

Fig. 8 The air mass flow rate at DB/WB= 2.0/0.8℃.

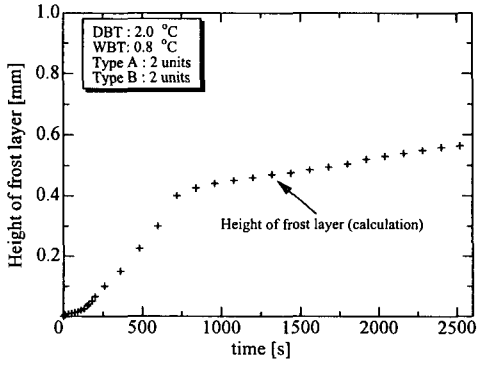

Fig. 9 The growth of the frost layer at DB/ WB=2.0/0.8℃.

calculated results and the experimental results of the condensing pressure and the evaporating pressure when two units of A type heat exchanger and two units of B type heat exchanger are used under 2.0/0.8℃ of dry-bulb and wet-bulb temperatures, respectively. Figure 6 shows the same comparison, when three units of A type heat exchanger, one unit of B type heat exchanger and one unit of C type heat exchanger are used under 2.0/1.5℃ of dry-bulb and wet-bulb temperatures, respectively.

When comparing the pressures in Fig. 6 to those in Fig. 4, there exists significant time delay until the pressures reach the minimum and maximum values from the start of operation. It means that when heating load increases, more time is needed until the system reaches the stable operation, where normal distribution of refrigerant occurs. Figure 6 also shows that the condensing and evaporating pressures drastically decrease comparing to those of Fig. 4, because saturated air could induce frost accumulation easily on spaces between fins, or between fin and tube.

Figures 5 and 7 show the change of heating capacity with time, under each operating condition. When starting operation, the predicted heating capacity is higher than measured one. When normal operation, the predicted one is lower than the measured one. Particularly, after reaching the maximum value, it shows that the predicted values show up to 25% lower than the measured one for about 2~5 minutes. It seems to be the same predicting results as the results of pressure changes that calculated in Figs. 4 and 6, and also it makes a good forecast for the phenomena that the more humidity involves in the conditions of air, the heating capacity decreases much faster. As shown in the characteristics of pressure (Figs. 4 and 6) and heating capacity (Figs. 5 and 7), the calculated results, comparing to experimental results, predict the overall tendency in a good manner. However the prediction is smaller than the experimental results, all for the condensing pressure, the evaporating pressure and the heating capacity. This reveals that the calculated results rapidly reflect the changes caused by the refrigerant movements in refrigerant side while calculating the prediction. The prediction is also affected by the factors such as thermal conductivity of frost layer, the changes of density of frost layer, various errors of experimental equations of correlation for the heat transfer and pressure drop, and the delay of heat quantity of the system, etc. However, causes of errors should be identified further as shown in the experimental values and calculation.

4.2 Air mass flow and the growth of frost layer

With the study of frosting phenomena, one

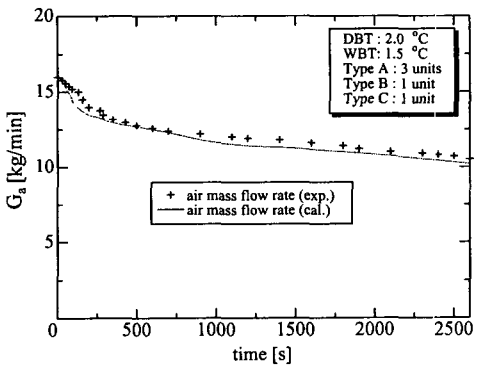

Fig. 10 The air mass flow rate at DB/WB= 2.0/1.5℃.

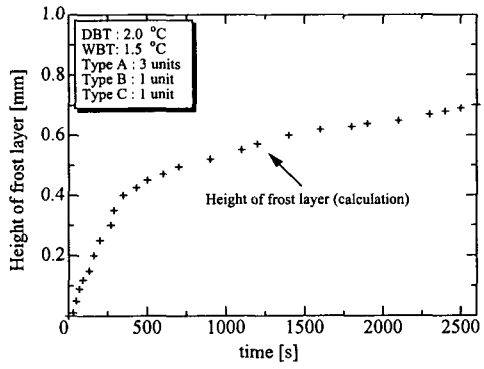

Fig. 11 The growth of the frost layer at DB/ WB=2.0/1.5℃.

of the most important subject to consider, together with the growth of frost layer, is the pressure drop in air side that closely relates to the growth of the frost layer. Figures 8 and 10 show the results of comparison of the air mass flow with the growth of the frost layer between experimental and calculated results under the same conditions as in the previous chapter, and Figs. 9 and 11 show the calculated growth rates of the frost layer. Especially, there are difficulties in experimentally measuring the growth of frost layers that occurs between fins, and between fin and tube. If air flow rate could be predicted with air-side pressure drop, it could be possible to treat the growth of frost layer as a geometric parameter that relates to the form of heat exchanger.

In Figs. 9 and 11, the frost layer grows with the start of the operation. Due to the reduction of airflow with this frost growth, the air mass flow is predicted to decrease gradually as shown in Figs. 8 and 10. As expected, the decreasing rates depended on the degree of humidity of air. The growth rate of the frost layer is also predicted to depend on the degree of humidity of air. However, in the actual system, the growth of frost layer was not detected upon starting the operation. It could be caused by the frosting model, as shown in Fig. 2, that the heat transfer coefficient and mass transfer coefficient are calculated independently. We assume that relationship between the heat transfer coefficient and the mass transfer coefficient need to be identified in a clearer manner in future. However, it predicts the air mass flow in air side very accurately, so that it shows a satisfactory result in terms of establishing techniques for the entire system design.

5. Conclusions

A new model was proposed for analyzing the heating performance of multi-inverter heat pumps considering frost accumulation on fin-tube type heat exchanger. We also build a simulation program with the developed model. With this model, we calculated the heat transfer coefficient and the mass transfer coefficient and applied it to the micro elements of each part of the heat exchanger. As this model depends on experimental values as basic parameters, it could bring about various restrictions and limits for actual applications. Nevertheless, the model could forecast the growth of frost, which is extremely difficult to measure when performing experiments. The model could also predict air-side pressure losses of heat exchangers, so that the model has a great advantage for further applications. We examined the feasibility of the simulation techniques and compared with experimental results, if not many. In addition, the developed program has input and output windows for easy access, and it will bring a great convenience to the users. If the relationship between the heat transfer coefficient and mass transfer coefficient could be verified, we believe that we could examine the frosting phenomena in a more simplified way. The frosting phenomena cause many bottlenecks and difficulties in designing air-conditioner heat pump, thus the efforts for developing performance analysis technique is to be continued.

References

1. Park, B. D., Chung, B. Y., Ha, D. Y. and Im, K. S., 1998, Development of simulation program for multi-airconditioner, Summer Conference of SRAEK, pp. 1370-1375.
2. Park, B. D., Lee, J. D., Koyama, Sh., Hwang, I. N., Chang, S. D. and Chung, B. Y., 2001, Development of the dynamic simulation program for the multi-inverter heat pump air-conditioner, Korean Journal of Air-Conditioning and Refrigeration Engineering, Vol. 13, No. 11, pp. 1079-1088.
3. Aoki, K., 1986, Frost formation and defrost-

ing for heat pump systems, Trans. of the JAR, Vol. 3, No. 2, pp. 1-9.
4. Aoki, K. and Hattori, M., 1990, Heat exchanger operating with frosting, Japanese Journal of Refrigeration, Vol. 65, No. 758, pp. 42-47.
5. Aoki, K., 1989, Characteristic on heat pump system due to frosting, Japanese Journal of Refrigeration, Vol. 64, No. 742, pp. 917-923.
6. Kim, C. H., Shin, J. M. and Ha, S. C., 2002, A study of frost formation on different hydrophilic surface, Korean Journal of Air-Conditioning and Refrigeration Engineering, Vol. 14, No. 6, pp. 519-524.
7. Choi, B. J. and Shin, J. M., 2002, The frost and defrost performance of fin-and-tube exchangers with different surface characteristics, Korean Journal of Air-Conditioning and Refrigeration Engineering, Vol. 14, No. 6, pp. 525-530.
8. Aoki, K., Hattori, M. and Akiyoshi, K., 1990, Characteristics of heat pump cycle with frosting, Proceeding of the 24th JAR, pp. 57-60.
9. Okawa, K., Tanaka, N. and Yoshino, Y. 1988, Analysis of heat and mass transfer of air cooling heat exchanger with frosting, Proceeding of the 22th JAR, pp. 49-52.
10. Ishihara, I., 1978, A study on heat transfer under frosting conditions, Ph.D. thesis, Kansai University, Osaka, Japan.
11. KSI, 1999, KSC9306, air conditioner, p. 44.